2018

An Axial Resistance-Varying Method for Improved Quantification of Enhanced Surface Condenser Tube Performance

Cameron Stuart Nelson
Johnson Controls, cameron.stuart.nelson@jci.com

Icksoo Kyung
Johnson Controls, icksoo.kyung@jci.com

An Axial Resistance-Varying Method for Improved Quantification of Enhanced Surface Condenser Tube Performance

Cameron S. NELSON[1]*, Icksoo KYUNG[1]

[1]Johnson Controls Advanced Development and Engineering Center
5000 Renaissance Drive, New Freedom, PA 17349, USA
*Phone: (717) 771-6245, E-mail: cameron.stuart.nelson@jci.com

* Corresponding Author

ABSTRACT

In shell-and-tube condensers, local heat flux and thermal resistance change along a tube's length due to the rise in water temperature as heat is absorbed. In this study, the outside heat transfer coefficient for pure condensation on an enhanced surface condenser tube was developed as a function of local heat flux. The developed heat transfer coefficient correlation was then substituted into the energy equation and solved to obtain the local mean water temperature as a function of axial position. The developed axial resistance-varying method was compared to the conventional log mean temperature difference method and showed applicability for long tube lengths where it better predicted water temperature approach and range.

1. INTRODUCTION: IMPACT OF LOCAL HEAT FLUX ON CONDENSATION HEAT TRANSFER

In industrial refrigeration, it is common for centrifugal chillers, in the range of 100 to 6,000 TR (352 to 21,100 kW), to utilize shell-and-tube heat exchangers. For the condenser shell-and-tube heat exchanger, the refrigerant occupies the shell-side, while the liquid (usually water or water-glycol mixture) occupies the tube-side. Condenser tubes are usually copper and utilize enhancements which are machined into the inside and outside cylindrical surfaces. They also typically have dimensions of either ¾″ or 1″ (19.1 or 25.4 mm) in diameter and are between 8 and 30 ft (2.44 and 9.14 m) long.

It is common in situations where two fluids exchange heat over an extended surface to apply the log mean temperature difference (LMTD) method because of its simplicity. For heat transfer between two co-current or cross-flowing fluids the LMTD method is written as,

$$q = UA\Delta T_{\mathrm{lm}} \tag{1}$$

where,

$$\Delta T_{\mathrm{lm}} = \frac{\Delta T_1 - \Delta T_2}{\ln(\Delta T_1/\Delta T_2)} \tag{2}$$

In the case of condensation with a pure refrigerant it is convenient to assume the refrigerant temperature away from the tube, or at the interface between the vapor and liquid phases, is constant and equal to the saturation temperature at the given condenser shell pressure.

Throughout the remainder of this paper, the condensation discussed will only concern itself with pure condensation, which is the case where the condenser tube is surrounded by stagnant vapor and is not affected by an impeding stream of condensate, known as inundation. The heat transfer diagram is therefore drawn as shown in Figure 1, where water enters on the left (at point 1), increases in temperature along the tube length as it absorbs heat from the condensing refrigerant, and leaves on the right (at point 2).

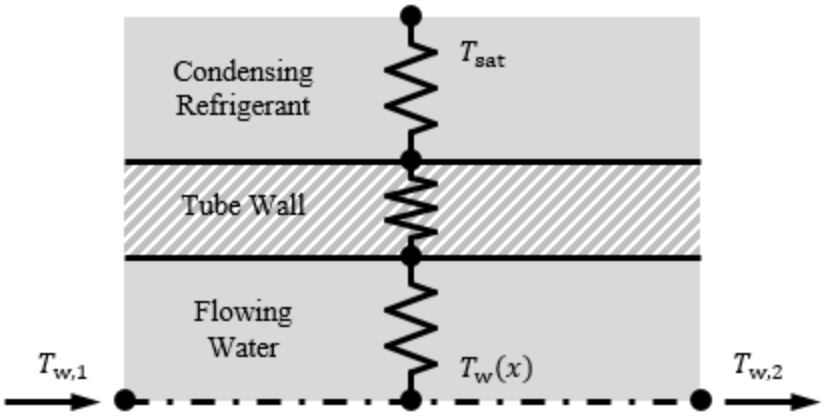

Figure 1: Pure condensation heat transfer diagram for outside condensation and internal liquid flow

Equations (1) and (2) can thus be re-written as,

$$q = UA\frac{T_{w,2} - T_{w,1}}{\ln\left(\left(T_{sat} - T_{w,1}\right)/\left(T_{sat} - T_{w,2}\right)\right)} \tag{3}$$

Conservation of energy on the water-side is,

$$q = \dot{m}_w c_{p,w}\left(T_{w,2} - T_{w,1}\right) \tag{4}$$

Re-arranging equation (3) and plugging in equation (4), the following equation is derived to solve explicitly for the exit mean water temperature, $T_{w,2}$.

$$T_{w,2} = T_{sat} + \left(T_{w,1} - T_{sat}\right)e^{-\frac{UA}{\dot{m}_w c_{p,w}}} \tag{5}$$

The assumptions applied to the LMTD method are that (1) the system is at steady-state, (2) the two fluids are adiabatically insulated from any outside body, resulting in heat transfer from the hot fluid to the cold fluid only, (3) no heat is conducted axially through either the tube or the fluids, (4) the potential and kinetic energy changes of the fluids are negligible, (5) the fluids' specific heats are constant, and (6) the overall heat transfer coefficient (HTC), U, is constant over the entire axial surface.

A consequence of applying the LMTD method is that the overall HTC is treated as constant for the entire tube length. For short tube lengths and/or high water flow rates where the water temperature does not change significantly, this practice is acceptable. However, if the tube length is long and/or water flow rates are low, the assumption of constant overall HTC can lead to inaccurate results. Heat flux is a strong function of the temperature difference between the refrigerant and the water. As the water temperature increases along the tube length, the heat flux will decrease roughly in proportion to the temperature difference. As the heat flux decreases, this causes a decrease in the amount of generated condensate on the outside surface of the condenser tube, resulting in a thinner condensate film thickness, and will therefore have a positive impact on the outside HTC (for heat fluxes below a drenching point).

The current study analyzes the impact of varying heat flux and outside HTC over the full length of a single enhanced surface condenser tube experiencing pure condensation. In other words, the local heat flux and the local HTC are treated as functions of x-position in order to properly fit the outside HTC correlation to experimental data. Furthermore, the resistance-varying method is developed to allow for the explicit solution of mean water temperature given the known boundary conditions and the local HTC correlation. Subsequently, the results from the LMTD method and the current resistance-varying method will be compared.

2. CONSERVATION OF ENERGY ON CONDENSER TUBE

To fairly account for variations in the heat flux and the inside and outside HTC's, these are developed in terms of their local values along all axial positions along a tube length. The conservation of energy differential equations for this problem, also shown in Figure 1, is written as,

$$q''(x) = \dot{m}_{\mathrm{w}} c_{p,\mathrm{w}} \frac{L}{A_{\mathrm{o}}} \frac{dT_{\mathrm{w}}}{dx}(x) \tag{6a}$$

and,

$$q''(x) = \frac{T_{\mathrm{sat}} - T_{\mathrm{w}}(x)}{\frac{A_{\mathrm{o}}}{h_{\mathrm{i}}(x) A_{\mathrm{i}}} + \frac{1}{h_{\mathrm{o}}(x)} + \frac{\ln(D_{\mathrm{r}}/D_{\mathrm{i}})\, A_{\mathrm{o}}}{2\pi k_{\mathrm{tube}} L} + R''_{\mathrm{f}} \frac{A_{\mathrm{o}}}{A_{\mathrm{i}}}} \tag{6b}$$

R''_{f} is the fouling factor for the inside tube surface and is considered to be zero for the tested tube since it was clean.

2.1 Simplification of the Inside HTC Correlation

The inside HTC is assumed to follow the Sieder-Tate correlation.

$$h_{\mathrm{i}}(x) = c_{\mathrm{ST}} \mathrm{Re}(x)^{0.8} \mathrm{Pr}(x)^{1/3} \left(\frac{\mu_{\mathrm{w}}(x)}{\mu_{\mathrm{wall}}(x)} \right)^{0.14} \tag{7}$$

As the correlation appears, there are several water properties that scale in unclear ways with respect to the water temperature. It would therefore be useful to re-write all of these terms as a simple function of mean water temperature. After further investigation, it is found that the water-side thermal resistance can be treated as a linear function of the mean water temperature as shown in Figure 2. This relation holds well for situations where the water flow does not transition between laminar and turbulent.

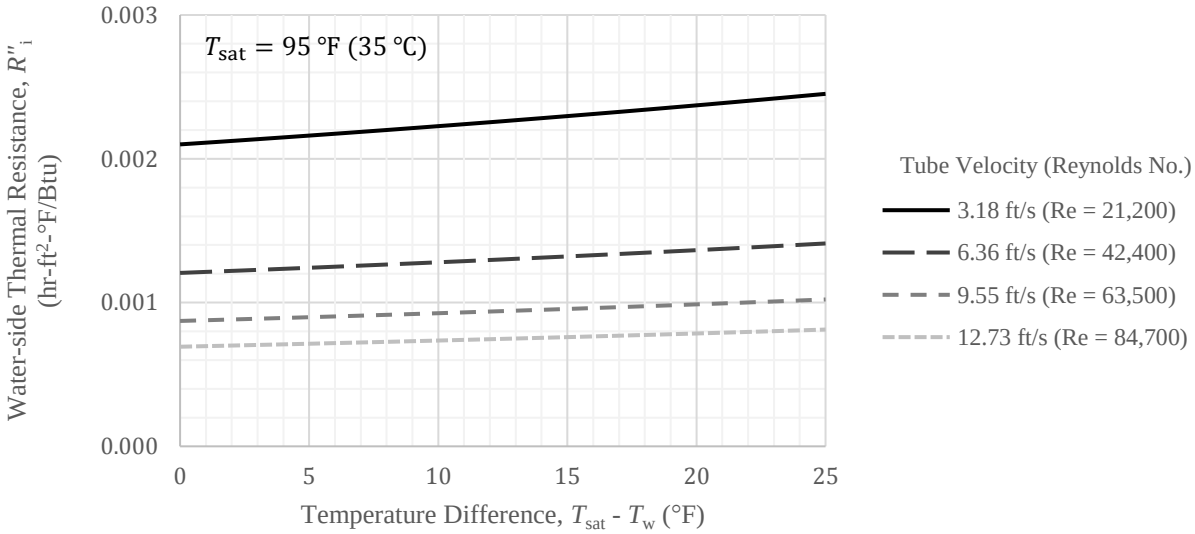

Figure 2: Relation of water-side thermal resistance to the mean water temperature

Conveniently, since the saturation temperature is a constant, the water resistance can be linearized as a function of the temperature difference. This allows for the following function to be developed where point 1 is at $x = 0$ (or $T_{\mathrm{w}} = T_{\mathrm{w},1}$) and point 2 is at $x = \infty$ (or $T_{\mathrm{w}} = T_{\mathrm{sat}}$).

$$\frac{1}{h_{\mathrm{i}}(T_{\mathrm{w}})} = \left(\frac{h_{\mathrm{i}}(T_{\mathrm{w},1})^{-1} - h_{\mathrm{i}}(T_{\mathrm{sat}})^{-1}}{T_{\mathrm{w},1} - T_{\mathrm{sat}}} \right) (T_{\mathrm{w}} - T_{\mathrm{sat}}) + \frac{1}{h_{\mathrm{i}}(T_{\mathrm{sat}})} \tag{8}$$

The final form of the local water-side HTC is written as,

$$\frac{1}{h_{\mathrm{i}}(x)} = R''_{\mathrm{grad}}\left(T_{\mathrm{sat}} - T_{\mathrm{w}}(x)\right) + R''_{\mathrm{sat}} \tag{10}$$

where,

$$R''_{\mathrm{grad}} = \frac{h_{\mathrm{i}}\left(T_{\mathrm{w},1}\right)^{-1} - h_{\mathrm{i}}(T_{\mathrm{sat}})^{-1}}{T_{\mathrm{sat}} - T_{\mathrm{w},1}} \tag{11}$$

$$R''_{\mathrm{sat}} = \frac{1}{h_{\mathrm{i}}(T_{\mathrm{sat}})} \tag{12}$$

2.2 Development of the Outside HTC Correlation

Pure condensation single tube heat transfer testing was conducted with a ¾″ (19.1 mm) diameter enhanced surface condenser tube that was 10 ft (3.05 m) long. Condenser vessel pressure, water flow rate, and water inlet and outlet temperatures were measured while varying the heat transfer rate and water flow rate through the tube. After processing the data and subtracting out the inside and wall resistances from the heat transfer path, the assumed constant outside HTC can be plotted against the average outside tube heat flux.

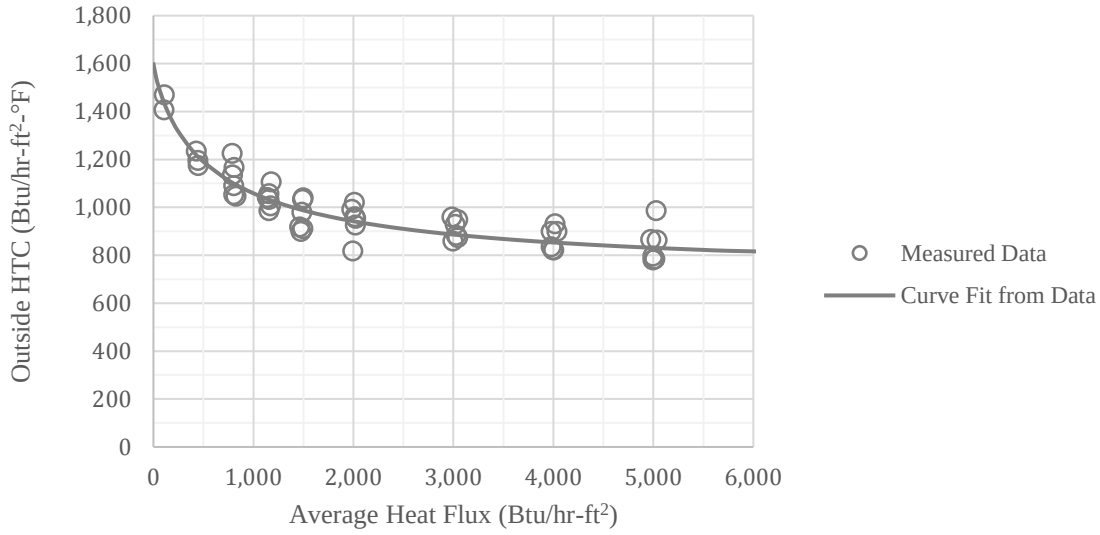

Figure 3: Outside HTC calculated from experimental data and LMTD method

The average heat flux, defined by the actual outside surface area, and the outside HTC were calculated using the following:

$$q''_{\mathrm{avg}} = \frac{\dot{m}_{\mathrm{w}} c_{p,\mathrm{w}}\left(T_{\mathrm{w},2} - T_{\mathrm{w},1}\right)}{A_{\mathrm{o}}} \tag{12}$$

$$h_{\mathrm{o}} = \left[\left\{\dot{m}_{\mathrm{w}} c_{p,\mathrm{w}} \ln\left(\frac{T_{\mathrm{sat}} - T_{\mathrm{w},1}}{T_{\mathrm{sat}} - T_{\mathrm{w},2}}\right)\right\}^{-1} - \frac{A_{\mathrm{o}}}{h_{\mathrm{i}}\left(T_{\mathrm{w,avg}}\right) A_{\mathrm{i}}} - \frac{\ln(D_{\mathrm{r}}/D_{\mathrm{i}})\, A_{\mathrm{o}}}{2\pi k_{\mathrm{tube}} L}\right]^{-1} \tag{13}$$

From the data shown in Figure 3, a curve fit may be applied using the LMTD method. While the solution, based on constant inside and outside HTC's, can be correlated well for the given 10 ft (3.05 m) tube, it can be seen clearly in the data that as the heat flux decreases the outside HTC increases due to a decrease in the generated condensate. Since heat flux is a strong function of the temperature difference, it is expected that for tubes where there is a large change in the water temperature that there will also be a significant difference in entering versus leaving heat flux. As a result, it is desirable to define the mean outside HTC as a function of x-position. For laminar film condensation

on the outside of a single smooth horizontal tube with stagnant surrounding vapor, Nusselt gives the following correlation:

$$h_{\mathrm{o,smooth}}(x) = 0.725\left[\frac{\rho_{\mathrm{L}}(\rho_{\mathrm{L}}-\rho_{\mathrm{V}})gk_{\mathrm{L}}^3}{D_{\mathrm{o}}\mu_{\mathrm{L}}}\left(\frac{\Delta h_{\mathrm{LV}}}{T_{\mathrm{sat}}-T_{\mathrm{wall}}(x)}+0.68c_{p,\mathrm{L}}\right)\right]^{1/4} \tag{14}$$

where the interfacial temperature is re-written as the saturation temperature. The adjustment to the latent heat is given by Rohsenow to account for the subcooling done by a condensing surface. The assumption of laminar film flow is strengthened in our case due to the presence of enhancements, which increase the wetted perimeter, and therefore reduce the Reynolds number of the film flow. Alternatively, a different correlation may be applied which is more applicable to enhanced surface condenser tubes such as a surface tension driven model rather than a gravity driven one. The following progression for the development of the resistance-varying method should yield similar results for either correlation.

For purposes of solving for an explicit closed form solution to the conservation of energy differential equation, it is important to write equation (14) in terms of heat flux. Knowing that, the heat transfer on the outside of the tube is characterized by,

$$q''(x) = h_{\mathrm{o,smooth}}(x)\left(T_{\mathrm{sat}}-T_{\mathrm{wall}}(x)\right) \tag{15}$$

equation (15) can be substituted into equation (14) to replace the temperature difference. Additionally, it is assumed that all fluid properties are close to those of the saturated liquid and vapor for the given uniform refrigerant pressure. Therefore,

$$h_{\mathrm{o,smooth}}(x) = (0.725)^{4/3}\left[\left.\frac{\rho_{\mathrm{L}}(\rho_{\mathrm{L}}-\rho_{\mathrm{V}})k_{\mathrm{L}}^3\Delta h_{\mathrm{LV}}}{\mu_{\mathrm{L}}}\right|_{\mathrm{sat}}\frac{g}{D_{\mathrm{o}}}\frac{1}{q''(x)}+0.68\left.\frac{\rho_{\mathrm{L}}(\rho_{\mathrm{L}}-\rho_{\mathrm{V}})k_{\mathrm{L}}^3c_{p,\mathrm{L}}}{\mu_{\mathrm{L}}}\right|_{\mathrm{sat}}\frac{g}{D_{\mathrm{o}}}\frac{1}{h_{\mathrm{o,smooth}}(x)}\right]^{1/3} \tag{16}$$

Referring back to equation (14), as the heat flux or temperature difference approaches infinity, the HTC will become,

$$h_{\mathrm{o,smooth}}(x)\big|_{q''\to\infty} = 0.725\left[0.68\left.\frac{\rho_{\mathrm{L}}(\rho_{\mathrm{L}}-\rho_{\mathrm{V}})k_{\mathrm{L}}^3c_{p,\mathrm{L}}}{\mu_{\mathrm{L}}}\right|_{\mathrm{sat}}\frac{g}{D_{\mathrm{o}}}\right]^{1/4} \tag{17}$$

Plugging this into equation (16) results in little error to the correlation since when the heat flux is low, the left term will dominate over the right. Additionally, two constants, c_1 and c_2, are added to scale the HTC with respect to the smooth tube case at medium and high heat fluxes respectively. To account for this properly, the smooth HTC is scaled proportionally with the nominal and actual outside areas in order to yield the outside HTC as defined. A heat flux constant, c_3, is also added to the local heat flux in the denominator since as the data indicates in Figure 3, the HTC will intercept the zero heat flux axis. Equation (16) is thus re-written as,

$$h_{\mathrm{o}}(x) = \left[\frac{(0.725c_1)^4\left.\frac{\rho_{\mathrm{L}}(\rho_{\mathrm{L}}-\rho_{\mathrm{V}})k_{\mathrm{L}}^3\Delta h_{\mathrm{LV}}}{\mu_{\mathrm{L}}}\right|_{\mathrm{sat}}\frac{g}{D_{\mathrm{o}}}+(0.725c_2)^3\left(0.68\left.\frac{\rho_{\mathrm{L}}(\rho_{\mathrm{L}}-\rho_{\mathrm{V}})k_{\mathrm{L}}^3c_{p,\mathrm{L}}}{\mu_{\mathrm{L}}}\right|_{\mathrm{sat}}\frac{g}{D_{\mathrm{o}}}\right)^{3/4}q''(x)}{c_3+q''(x)}\right]^{1/3}\frac{\pi D_{\mathrm{o}}L}{A_{\mathrm{o}}} \tag{18}$$

Once again, the addition of c_3 should have minimal effect on the correlation at medium to high heat fluxes since the heat flux term will dominate over the added constant. This allows the HTC correlation to follow the one-third power at medium to high heat fluxes while also producing a fixed HTC at zero heat flux. To simplify this very long equation, the following is defined:

$$a = (0.725c_1)^4\left.\frac{\rho_{\mathrm{L}}(\rho_{\mathrm{L}}-\rho_{\mathrm{V}})k_{\mathrm{L}}^3\Delta h_{\mathrm{LV}}}{\mu_{\mathrm{L}}}\right|_{\mathrm{sat}}\frac{g}{D_{\mathrm{o}}}\left(\frac{\pi D_{\mathrm{o}}L}{A_{\mathrm{o}}}\right)^3 \tag{19}$$

$$b = (0.725c_2)^3\left(0.68\left.\frac{\rho_{\mathrm{L}}(\rho_{\mathrm{L}}-\rho_{\mathrm{V}})k_{\mathrm{L}}^3c_{p,\mathrm{L}}}{\mu_{\mathrm{L}}}\right|_{\mathrm{sat}}\frac{g}{D_{\mathrm{o}}}\right)^{3/4}\left(\frac{\pi D_{\mathrm{o}}L}{A_{\mathrm{o}}}\right)^3 \tag{20}$$

Therefore,

$$h_{\mathrm{o}}(x) = \left(\frac{a + bq''(x)}{c_3 + q''(x)}\right)^{1/3} \tag{21}$$

With the conclusion of the definition of the inside and outside HTC correlations, equation (6b) can now be re-written with equations (10) and (21) as,

$$q''(x) = \frac{T_{\mathrm{sat}} - T_{\mathrm{w}}(x)}{\left(R''_{\mathrm{grad}}\left(T_{\mathrm{sat}} - T_{\mathrm{w}}(x)\right) + R''_{\mathrm{sat}}\right)\frac{A_{\mathrm{o}}}{A_{\mathrm{i}}} + \left(\frac{c_3 + q''(x)}{a + bq''(x)}\right)^{1/3} + \frac{\ln(D_{\mathrm{r}}/D_{\mathrm{i}})\,A_{\mathrm{o}}}{2\pi k_{\mathrm{tube}} L} + R''_{\mathrm{f}}\frac{A_{\mathrm{o}}}{A_{\mathrm{i}}}} \tag{22}$$

2.3 Altering the Differential Equation to a Solvable Form

To simplify equations (6a) and (22), let's define the following:

$$k_q = \dot{m}_{\mathrm{w}} c_{p,\mathrm{w}} \frac{L}{A_{\mathrm{o}}} \tag{23}$$

$$R''_{\mathrm{g}} = R''_{\mathrm{grad}} \frac{A_{\mathrm{o}}}{A_{\mathrm{i}}} \tag{24}$$

$$R''_{\mathrm{c}} = R''_{\mathrm{sat}} \frac{A_{\mathrm{o}}}{A_{\mathrm{i}}} + \frac{\ln(D_{\mathrm{r}}/D_{\mathrm{i}})\,A_{\mathrm{o}}}{2\pi k_{\mathrm{tube}} L} + R''_{\mathrm{f}} \frac{A_{\mathrm{o}}}{A_{\mathrm{i}}} \tag{25}$$

$$\theta = T_{\mathrm{w}}(x) - T_{\mathrm{sat}} \tag{26}$$

$$\frac{d\theta}{dx} = \frac{dT_{\mathrm{w}}}{dx}(x) \tag{27}$$

Equation (6a) is re-written as,

$$q''(x) = k_q \frac{d\theta}{dx} \tag{28}$$

By plugging equations (23) through (28) into equation (22), the conservation of energy differential equation (which is first-order, nonlinear, and ordinary) is thus written in its final form as,

$$k_q \frac{d\theta}{dx} = \frac{-\theta}{-R''_{\mathrm{g}}\theta + \left(\frac{c_3 + k_q \frac{d\theta}{dx}}{a + bk_q \frac{d\theta}{dx}}\right)^{1/3} + R''_{\mathrm{c}}} \tag{29}$$

2.4 Solution to the Conservation of Energy Differential Equation

The exact solution follows as,

$$\theta = -\frac{R''_{\mathrm{o},\theta} + R''_{\mathrm{c}}}{B_\theta} k_q \frac{d\theta}{dx} \tag{30a}$$

and,

$$\frac{d^2\theta}{dx^2} = -B_\theta \left[\frac{R''_{\mathrm{o},\theta} + R''_{\mathrm{c}}}{B_\theta} + \frac{a}{3C_\theta^3}\left(R''_{\mathrm{o},\theta} - \frac{c_3}{a{R''_{\mathrm{o},\theta}}^2}\right)\right]^{-1} \frac{1}{k_q}\frac{d\theta}{dx} \tag{30b}$$

where,

$$R''_{\mathrm{o},\theta} = \left(\frac{c_3 + k_q \frac{d\theta}{dx}}{a + bk_q \frac{d\theta}{dx}}\right)^{1/3} \tag{31}$$

$$B_\theta = 1 - k_q R''_{\mathrm{g}} \frac{d\theta}{dx} \tag{32}$$

$$C_\theta = \left(a + b k_q \frac{d\theta}{dx}\right)^{1/3} \tag{33}$$

Given the complexity of equations (30a) and (30b), it is necessary to approximate the solution and discretize to yield accurate results. In this situation where $\frac{d^2\theta}{dx^2}$ can be solved as a function of $\frac{d\theta}{dx}$, the Runge-Kutta method, which is 4$^{\text{th}}$-order accurate, becomes very useful for solving for $\left.\frac{d\theta}{dx}\right|_{n+1}$ at $x = x_{n+1}$.

Knowing the initial water temperature, $\left.\frac{d\theta}{dx}\right|_{n=1}$ can be iteratively solved for with,

$$\left.\frac{d\theta}{dx}\right|_{n=1} = \left.\frac{B_\theta}{R''_{\mathrm{o},\theta} + R''_{\mathrm{c}}}\right|_{n=1} \frac{\left(T_{\mathrm{sat}} - T_{\mathrm{w},n=1}\right)}{k_q} \tag{34}$$

The Runge-Kutta coefficients are solved using:

$$k_1 = \frac{d^2\theta}{dx^2}\left(\left.\frac{d\theta}{dx}\right|_n\right) \tag{35a}$$

$$k_2 = \frac{d^2\theta}{dx^2}\left(\left.\frac{d\theta}{dx}\right|_n + \frac{1}{2}\Delta x_n k_1\right) \tag{35b}$$

$$k_3 = \frac{d^2\theta}{dx^2}\left(\left.\frac{d\theta}{dx}\right|_n + \frac{1}{2}\Delta x_n k_2\right) \tag{35c}$$

$$k_4 = \frac{d^2\theta}{dx^2}\left(\left.\frac{d\theta}{dx}\right|_n + \Delta x_n k_3\right) \tag{35d}$$

The Runge-Kutta solution to the conservation of energy differential equation is thus,

$$\left.\frac{d\theta}{dx}\right|_{n+1} = \left.\frac{d\theta}{dx}\right|_n + \frac{1}{6}\Delta x_n (k_1 + 2k_2 + 2k_3 + k_4) \tag{36}$$

and,

$$x_{n+1} = x_n + \Delta x_n \tag{37}$$

Re-writing equation (30a), the local mean water temperature at x_{n+1} is solved with,

$$T_{\mathrm{w},n+1} = T_{\mathrm{sat}} - \left.\frac{R''_{\mathrm{o},\theta} + R''_{\mathrm{c}}}{B_\theta}\right|_{n+1} k_q \left.\frac{d\theta}{dx}\right|_{n+1} \tag{38}$$

Additionally, the local heat flux and local outside HTC can be solved at any axial position using equations (28) and (21) respectively. Equations (31) through (38) can be written into a short program in order to explicitly solve for mean water temperature as a function of x-position given inlet water flow and properties, condenser saturation temperature, the coefficients for the inside and outside HTC correlations, the tube wall thermal resistance, and the tube geometry. To verify that a small enough discretization step is being used, simply reduce the step size and the simplified solution to equation (30a) and (30b) will converge to a solution at a 4$^{\text{th}}$-order convergence rate.

3. COMPARISON OF RESISTANCE-VARYING METHOD TO LMTD

Using the data shown in Figure 3 and the above solution method with discretized segment lengths of 1.2 in, the total tube heat rate (using exit water temperature) was solved for and compared against the actual total tube heat rate while iteratively changing the three correlation constants until the best fit of the correlation to the experimental data was achieved. The local outside HTC correlation against local heat flux is shown with the black line in Figure 4. The standard deviation on the percent difference between the solution heat rate and the data heat rate was 1.33 % difference for constant values of $c_1 = 4.810$, $c_2 = 19.609$, and $c_3 = 287$ Btu/hr-ft^2 (905 W/m^2).

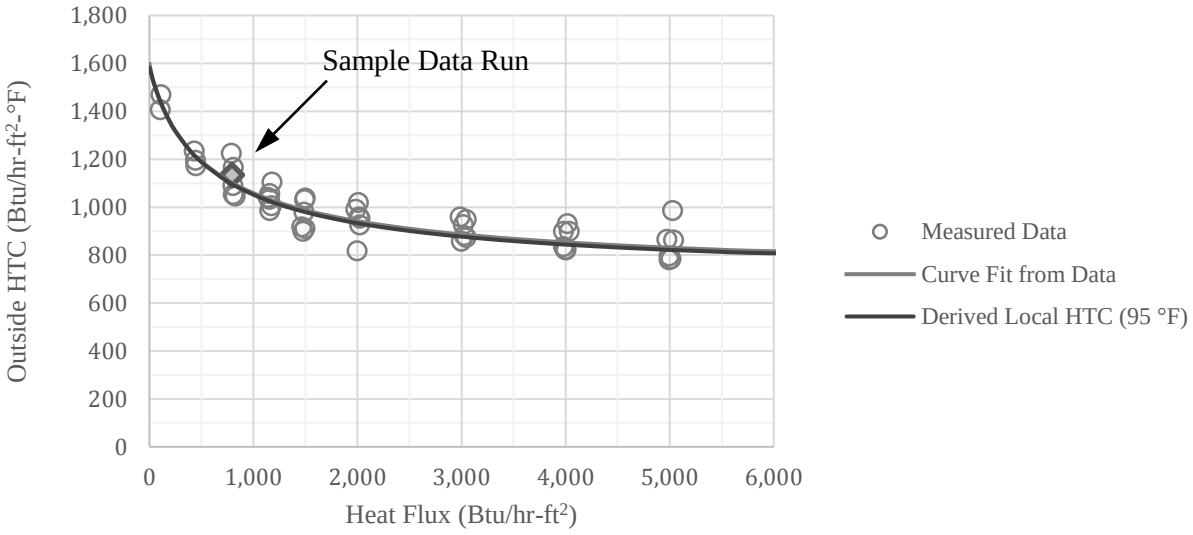

Figure 4: Derived local HTC at a saturation temperature of 95 °F (35 °C) as a function of local heat flux using resistance-varying method applied over entire tube length

Using an example sample data run (shown by the gray diamond in Figure 4), the resistance-varying method allows for the calculation of the mean water temperature, heat flux, and outside HTC as functions of x-position.

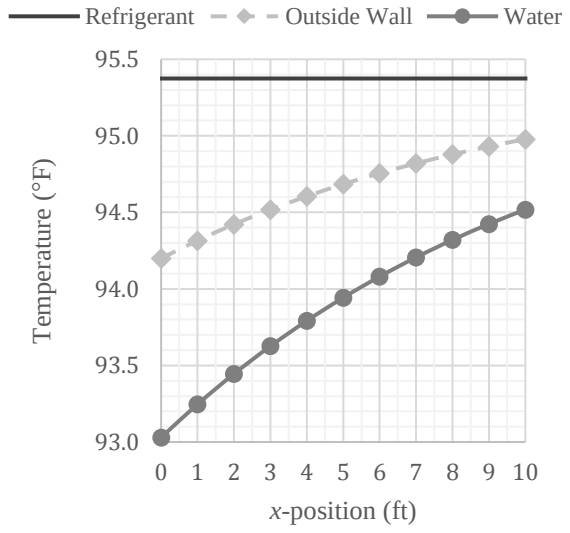

Figure 5: Sample refrigerant and mean water temperature profiles using the resistance-varying method

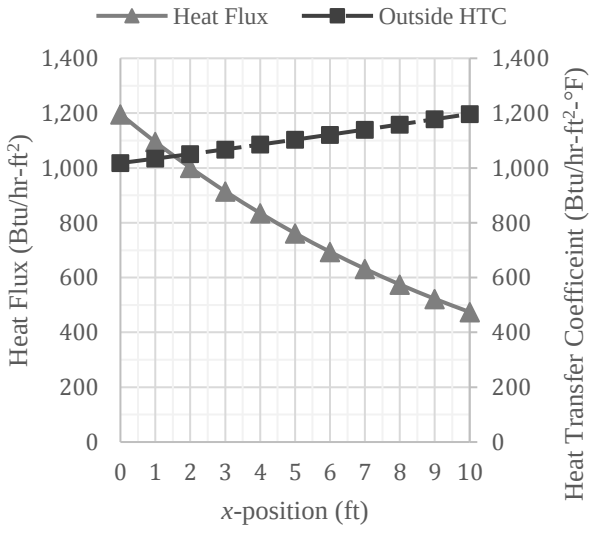

Figure 6: Sample heat flux and HTC profiles using the resistance-varying method

As shown in Figures 5 and 6, the outside HTC can increase by 20 % from the entrance to the exit of the 10 ft (3.05 m) long tube.

For long tubes with large incoming temperature differences, the maximum possible HTC increase would be,

$$\frac{h_{\mathrm{o}}|_{q_{\mathrm{o}}''=0}}{h_{\mathrm{o}}|_{q_{\mathrm{o}}''\to\infty}} - 1 = \frac{0.725^{1/3} c_1^{4/3}}{0.68^{1/4} c_2 c_3^{1/3}} \left[\left. \frac{\rho_{\mathrm{L}}(\rho_{\mathrm{L}} - \rho_{\mathrm{V}}) k_{\mathrm{L}}^3}{\mu_{\mathrm{L}}} \right|_{\mathrm{sat}} \frac{g}{D_{\mathrm{o}}} \right]^{1/12} \left. \frac{\Delta h_{\mathrm{LV}}^{1/3}}{c_{p,\mathrm{L}}^{1/4}} \right|_{\mathrm{sat}} - 1 \tag{39}$$

at a given saturation temperature. For pure condensation at a saturation temperature of 95 °F (35 ℃) on the given tube, the maximum possible outside HTC increase is 123 %. The equivalent change in thermal resistance is a decrease of 55 %.

The LMTD method is compared to the resistance-varying method using the derived local HTC correlation mentioned above for both. (See Figures 7 and 8) This analysis was based on an entering water temperature of 85 °F (29.4 ℃) and an entering water velocity of 6.35 ft/s (1.94 m/s), or 50 $\mathrm{lb_m/min}$ (0.38 kg/s). The LMTD method determined the assumed constant inside and outside HTC's based on the average water temperature and the average heat flux respectively.

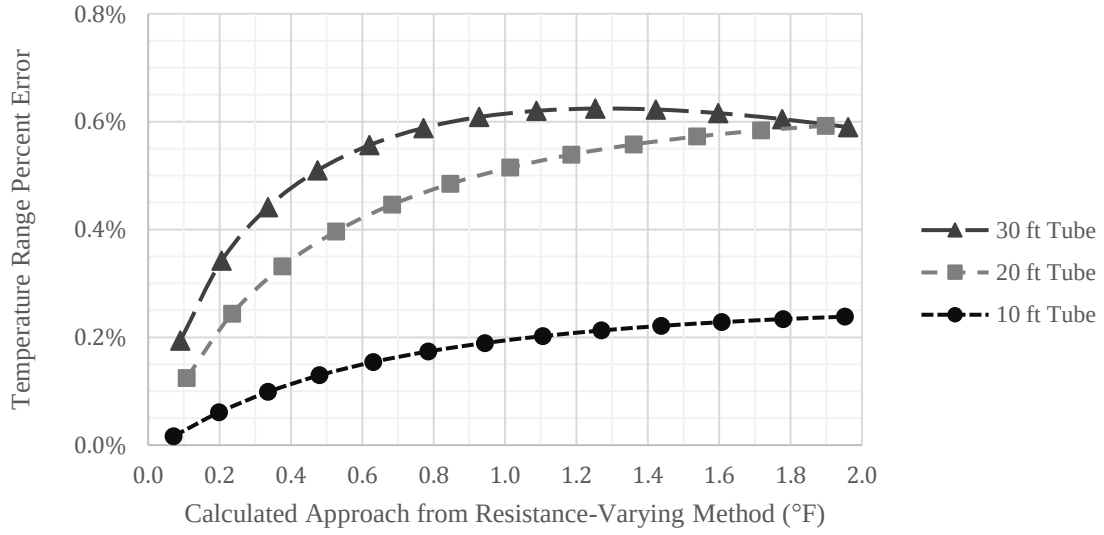

Figure 7: Temperature range percent error for LMTD compared to the resistance-varying method

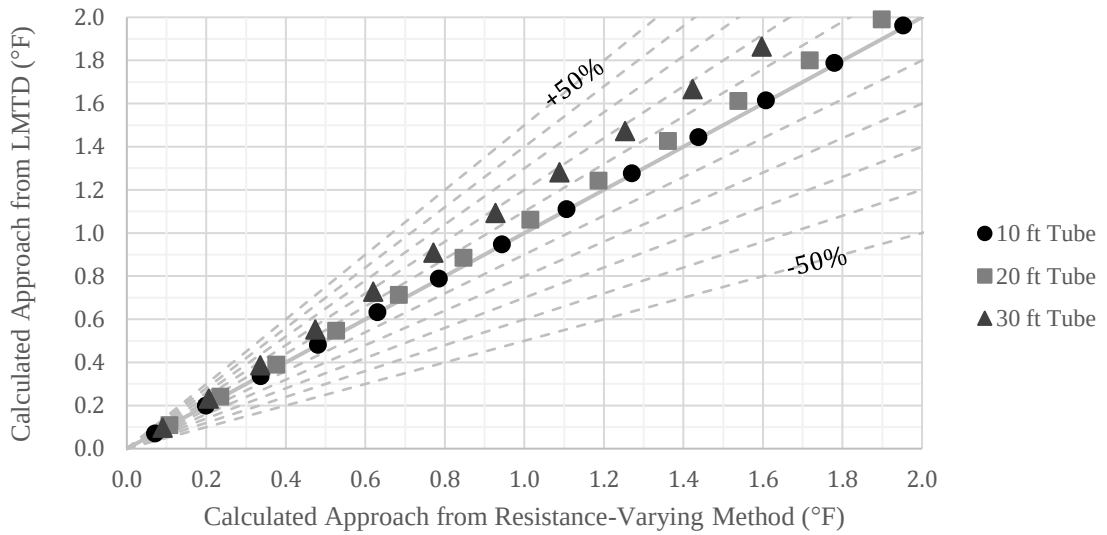

Figure 8: Approach percent error for LMTD compared to the resistance-varying method

It is observed that the error for the 10 ft (3.05 m) long tube is small and that the LMTD method produces good results. However, as the tube length increases, the error grows, thus making the resistance-varying method more attractive for predicting accurate performance. As shown, the LMTD method produces an error for the water temperature range (or total heat removed) of up to 0.6 % for the 30 ft (9.14 m) long tube. Additionally, the approach temperature error can be up to approximately +0.25 °F (+0.14 °C), or +18 % error.

4. DISCUSSION AND CONCLUSIONS

As it has been seen, the axial resistance-varying method for pure condensation on enhanced surface condenser tubes produces more accurate results than the LMTD method due to its ability to account for changes in the inside and outside HTC's along the tube length. This is especially evident for long condenser tubes where the mean water temperature varies notably from inlet to outlet. In general, as the tube length increases, errors in the water temperature approach and range increase. Since individual tube experimental data is typically taken with short tube lengths, it is highly useful to interpret results to predict phenomena at any axial position, and from that appropriately fine-tune correlation coefficients. In this manner, performance of a condenser tube of any length may be known.

In addition, an explicit closed-form solution to the mean water temperature, heat flux, and outside HTC as functions of position through the tube were obtained, to allow for quantification of heat transfer characteristics over the condensation surface. This was achievable, by linearization of the Sieder-Tate correlation, scaling and fine-adjustment of the Nusselt correlation, and simplification of the conservation of energy differential equation with the Runge-Kutta 4th-order accurate numerical discretization method in order to yield the explicit closed-form solution.

Future work in this area could involve further experimentation with pure condensation at other saturation temperatures to verify that the correlation given by Nusselt for laminar film condensation on a horizontal tube appropriately applies to the enhanced surface condenser tube. In the event that it does not, a correlation including surface tension or other effects may need applied instead. Testing could also be conducted to properly quantify the subcooling effect given by Rohsenow. Moreover, this approach may be extended to an entire horizontal shell-and-tube heat exchanger where more complex effects such as inundation, vapor shear, and pressure drop over the tube bank may need accounted for in order to accurately model and predict full condenser heat exchanger performance.

NOMENCLATURE

Symbol	Description	English units	SI units
A	Area of a heat transfer surface	ft^2	m^2
A_i	Actual inside surface area of tube	ft^2	m^2
A_o	Actual outside surface area of tube	ft^2	m^2
a	Constant a	$\mathrm{Btu}^4/\mathrm{hr}^4\text{-ft}^8\text{-}^\circ\mathrm{F}^3$	$\mathrm{W}^4/\mathrm{m}^8\text{-K}^3$
B_θ	B_θ function	–	–
b	Constant b	$\mathrm{Btu}^3/\mathrm{hr}^3\text{-ft}^6\text{-}^\circ\mathrm{F}^3$	$\mathrm{W}^3/\mathrm{m}^6\text{-K}^3$
C_θ	C_θ function	$(\mathrm{Btu/hr\text{-}ft}^2)^{4/3}/^\circ\mathrm{F}$	$(\mathrm{W/m}^2)^{4/3}/\mathrm{K}$
c_ST	Sieder-Tate constant	–	–
$c_\mathrm{p,L}$	Specific heat of liquid refrigerant	$\mathrm{Btu/lb_m\text{-}^\circ F}$	kJ/kg-K
$c_\mathrm{p,w}$	Specific heat of water at mean temperature	$\mathrm{Btu/lb_m\text{-}^\circ F}$	kJ/kg-K
c_1	Scaling factor at medium heat fluxes	–	–
c_2	Scaling factor at high heat fluxes	–	–
c_3	Offset heat flux coefficient	$\mathrm{Btu/hr\text{-}ft}^2$	$\mathrm{W/m}^2$
D_i	Inside Diameter	in	mm
D_o	Outside Diameter	in	mm
D_r	Root Diameter	in	mm
g	Acceleration due to gravity	$\mathrm{ft/s}^2$	$\mathrm{m/s}^2$
h_i	Inside heat transfer coefficient	$\mathrm{Btu/hr\text{-}ft}^2\text{-}^\circ\mathrm{F}$	$\mathrm{W/m}^2\text{-K}$
h_o	Outside heat transfer coefficient	$\mathrm{Btu/hr\text{-}ft}^2\text{-}^\circ\mathrm{F}$	$\mathrm{W/m}^2\text{-K}$
Δh_LV	Latent heat at thermodynamic equilibrium	$\mathrm{Btu/lb_m}$	kJ/kg
k_L	Thermal conductivity of liquid refrigerant	Btu/hr-ft-°F	W/m-K
k_q	Water flow heat capacity per actual outside circumference	Btu/hr-ft-°F	W/m-K
k_tube	Thermal conductivity of the tube wall	Btu/hr-ft-°F	W/m-K
k_1	Runge-Kutta coefficient 1	$^\circ\mathrm{F/ft}^2$	$^\circ\mathrm{C/m}^2$
k_2	Runge-Kutta coefficient 2	$^\circ\mathrm{F/ft}^2$	$^\circ\mathrm{C/m}^2$
k_3	Runge-Kutta coefficient 3	$^\circ\mathrm{F/ft}^2$	$^\circ\mathrm{C/m}^2$
k_4	Runge-Kutta coefficient 4	$^\circ\mathrm{F/ft}^2$	$^\circ\mathrm{C/m}^2$
L	Length of tube	ft	m
$\dot{m}_\mathrm{w}$	Water mass flow rate	$\mathrm{lb_m/min}$	kg/s
$_n$	n-step in discretization	–	–
Pr	Prandtl number	–	–
q	Total heat rate	Btu/hr	W
q''	Heat flux	$\mathrm{Btu/hr\text{-}ft}^2$	$\mathrm{W/m}^2$
q''_avg	Average heat flux	$\mathrm{Btu/hr\text{-}ft}^2$	$\mathrm{W/m}^2$
R''_c	Total constant resistance	$\mathrm{hr\text{-}ft}^2\text{-}^\circ\mathrm{F/Btu}$	$\mathrm{m}^2\text{-K/W}$
R''_f	Fouling factor (on inside surface)	$\mathrm{hr\text{-}ft}^2\text{-}^\circ\mathrm{F/Btu}$	$\mathrm{m}^2\text{-K/W}$
R''_g	Constant gradient resistance	$\mathrm{hr\text{-}ft}^2/\mathrm{Btu}$	m^2/W
R''_grad	Constant gradient resistance on inside surface	$\mathrm{hr\text{-}ft}^2/\mathrm{Btu}$	m^2/W
R''_i	Water-side resistance	$\mathrm{hr\text{-}ft}^2\text{-}^\circ\mathrm{F/Btu}$	$\mathrm{m}^2\text{-K/W}$

Symbol	Description	English units	SI units
$R''_{o,\theta}$	Refrigerant-side thermal resistance	hr-ft^2-°F/Btu	m^2-K/W
R''_{sat}	Water-side res. on inside surface at saturation temperature	hr-ft^2-°F/Btu	m^2-K/W
Re	Reynolds number	–	–
T_{sat}	Saturation temperature of the refrigerant	°F	°C
T_w	Mean water temperature	°F	°C
$T_{w,1}$	Mean water temperature at point 1 (entering)	°F	°C
$T_{w,2}$	Mean water temperature at point 2 (leaving)	°F	°C
T_{wall}	Inside surface wall temperature	°F	°C
ΔT_{lm}	Log mean temperature difference	°F	°C
ΔT_1	Temperature difference at point 1	°F	°C
ΔT_2	Temperature difference at point 2	°F	°C
$\frac{dT_w}{dx}$	Differential of mean water temperature with x-position	°F/ft	°C/m
U	Overall heat transfer coefficient	Btu/hr-ft^2-°F	W/m^2-K
x	Axial or longitudinal position along tube	ft	m
Δx	Discrete length	ft	m
θ	Temperature difference between saturated refr. and water	°F	°C
$\frac{d\theta}{dx}$	First derivative of θ with respect to x-position	°F/ft	°C/m
$\frac{d^2\theta}{dx^2}$	Second derivative of θ with respect to x-position	°F/ft^2	°C/m^2
μ_L	Viscosity of the liquid refrigerant	lb$_m$/ft-hr	μPa-s
μ_w	Viscosity of water at mean temperature	lb$_m$/ft-hr	μPa-s
μ_{wall}	Viscosity of water on wall surface	lb$_m$/ft-hr	μPa-s
ρ_L	Density of the liquid refrigerant	lb$_m$/ft^3	kg/m^3
ρ_V	Density of the vapor refrigerant	lb$_m$/ft^3	kg/m^3

REFERENCES

Incropera F. P., Dewitt D. P., Bergman T. L., Lavine A. S. (2011). *Fundamentals of Heat and Mass Transfer* (7th ed.). Jefferson City, MO: John Wiley & Sons.

Kutta, M. W. (1901). *Beitrag zur näherungweisen Integration totaler Differentialgleichungen*.

Nusselt, W. (1916). Die Oberflächenkondensation des Wasserdampfes. *Zeitschrift des Vereines Deutscher Ingenieure*., **60**(27), 541, 569.

Rohsenow, W. M. (1956). Heat transfer and temperature distribution in laminar film condensation. *Trans. ASME*, **79**, 1645-1648.

Runge, C. D. T. (1895). Über die numerische Auflösung von Differentialgleichungen. *Mathematische Annalen*, **46**(2), 167-178.